Available online at www.sciencedirect.com
SCIENCE DIRECT
Journal of Sound and Vibration 296 (2006) 554–566
JOURNAL OF SOUND AND VIBRATION
www.elsevier.com/locate/jsvi

Study on localization of plane elastic waves in disordered periodic 2–2 piezoelectric composite structures

Feng-Ming Li*, Yue-Sheng Wang

Institute of Engineering Mechanics, School of Civil Engineering, Beijing Jiaotong University, Beijing 100044, People's Republic of China

Received 2 June 2004; received in revised form 23 May 2005; accepted 31 January 2006
Available online 5 June 2006

Abstract

Considering the effect of mechanic–electric coupling, the propagation and localization of plane elastic waves in disordered periodic layered piezoelectric composite structures are studied. The transfer matrix between two consecutive unit cells is obtained by means of the continuity conditions and the expression of the localization factors in disordered periodic structures is presented by regarding the variables of mechanical and electrical fields as the elements of state vectors. As examples, numerical results of localization factors are presented and discussed. It can be seen from the results that ordered periodic structures possess the properties of frequency passbands and stopbands and the phenomenon of wave localization in disordered periodic structures is observed, and the larger the coefficient of variation is, the larger the localization factor or the stronger the degree of wave localization is. The characters of wave propagation and localization are very different for different sorts of piezocomposites or different structural sizes, and even for same sorts of piezocomposites and same structural sizes the characters of wave propagation and localization are also very different for different non-dimensional wavenumbers. We may design different piezocomposites or adjust the structural sizes to control the characters of wave propagation and localization.

1. Introduction

The capabilities of self-adaptive and active control are the main characters for intelligent materials and structures which can perceive the changes of outer environment and properly respond to these changes and therefore are extensively used in many engineering applications [1]. Presently, piezoelectric composites which are made up of piezoelectric ceramics and polymers are more and more used among various intelligent materials, especially, in aeronautic and astronautic engineering. Piezocomposites not only possess the merits of both piezoceramics and polymers but also greatly enhance the piezoelectric performances of the materials and will accordingly become the main study and application domain in the development of future intelligent materials and structures.

For some special using purposes, many piezoelectric components and structures have periodicity and various periodic piezoelectric composites are extensively employed in intelligent materials and structures [2–4].

*Corresponding author.
E-mail address: llffcc@tom.com (F.-M. Li).

0022-460X/$ - see front matter © 2006 Elsevier Ltd. All rights reserved.
doi:10.1016/j.jsv.2006.01.057

Different from non-periodic engineering structures, periodic ones have many special dynamical characters such as frequency passband and stopband [5]. Disordered periodic structures can also exhibit wave and vibration localization characters [6–8]. Localization leads to spatial decay of wave amplitudes, and the associated exponential decay constant is known as the localization factor which characterizes the average exponential rates of decay of wave amplitudes in disordered periodic structures. Due to the special dynamic characters of periodic and disordered periodic structures, many people have studied this problem [9,10].

In previous studies on the problem of wave and vibration localization, most people considered the case of pure elastic disordered periodic structures and disordered periodic piezocomposites are seldom studied. Only Baz [5] and Thorp et al. [6] investigated the problems of active vibration control and wave localization in periodic spring–mass systems controlled by piezoelectric actuators and rods with periodic shunted piezoelectric patches and drew some significant conclusions. Dynamic loads are often met in practical engineerings, which makes it necessary to study wave propagation and localization in disordered periodic piezoelectric composite structures.

In this study, the problem of wave propagation and localization are studied in disordered periodic 2–2 piezoelectric composite structures. The mechanical and electrical coupling characters of piezoelectric composite materials are considered. The transfer matrix between two consecutive unit cells is obtained by means of the continuity conditions. Regarding the variables of mechanical and electrical fields as the elements of state vectors, the formulation for calculating localization factor in disordered periodic structures is presented. By introducing disorder, wave localization in the mistuned periodic structures is analyzed.

2. Equations of wave motion

A periodic 2–2 piezoelectric composite structure is shown in Fig. 1. The periodic layered structure consists of polymeric and piezoelectric thin films alternately. Assuming that the thickness of polymers and that of piezoelectric ceramics are a_1 and a_2. The local coordinates of polymeric film and those of piezoelectric film are also displayed in Fig. 1.

For the problem of plane strain, the constitutive equations of the polymers and the transversely isotropic piezoelectric ceramics can be expressed as follows [11,12]:

$$\sigma_{xxj} = c_{11}^{(j)} \frac{\partial u_{xj}}{\partial x_j} + c_{13}^{(j)} \frac{\partial u_{zj}}{\partial z_j} + e_{13}^{(j)} \frac{\partial \varphi_j}{\partial z_j}, \tag{1a}$$

$$\sigma_{zzj} = c_{13}^{(j)} \frac{\partial u_{xj}}{\partial x_j} + c_{33}^{(j)} \frac{\partial u_{zj}}{\partial z_j} + e_{33}^{(j)} \frac{\partial \varphi_j}{\partial z_j}, \tag{1b}$$

$$\sigma_{xzj} = c_{44}^{(j)} \frac{\partial u_{xj}}{\partial z_j} + c_{44}^{(j)} \frac{\partial u_{zj}}{\partial x_j} + e_{15}^{(j)} \frac{\partial \varphi_j}{\partial x_j}, \tag{1c}$$

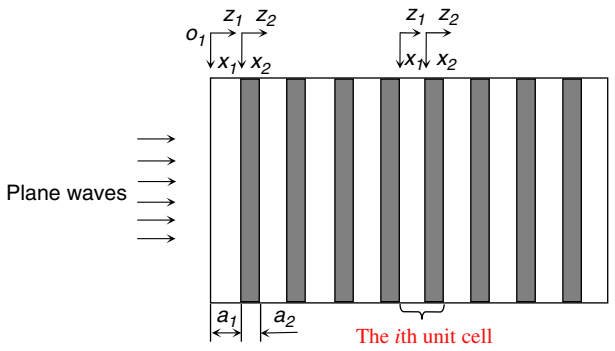

Fig. 1. Schematic diagram of a periodic 2–2 piezoelectric composite structure.

$$D_{xj} = e_{15}^{(j)} \frac{\partial u_{xj}}{\partial z_j} + e_{15}^{(j)} \frac{\partial u_{zj}}{\partial x_j} - \varepsilon_{11}^{(j)} \frac{\partial \varphi_j}{\partial x_j}, \tag{1d}$$

$$D_{zj} = e_{13}^{(j)} \frac{\partial u_{xj}}{\partial x_j} + e_{33}^{(j)} \frac{\partial u_{zj}}{\partial z_j} - \varepsilon_{33}^{(j)} \frac{\partial \varphi_j}{\partial z_j} \quad (j = 1, 2), \tag{1e}$$

where $u_{xj}(x_j, z_j, t)$ and $u_{zj}(x_j, z_j, t)$ are the displacements in the x and z directions, $\varphi_j(x_j, z_j, t)$ the electric potential functions, σ_{xxj}, σ_{zzj} and σ_{xzj} the stresses, D_{xj} and D_{zj} the electric displacements, $c_{11}^{(j)}$, $c_{13}^{(j)}$, $c_{33}^{(j)}$ and $c_{44}^{(j)}$ the elastic constants, $e_{13}^{(j)}$, $e_{33}^{(j)}$ and $e_{15}^{(j)}$ the piezoelectric constants, and $\varepsilon_{11}^{(j)}$ and $\varepsilon_{33}^{(j)}$ the dielectric constants, with $j = 1$ referring to the polymers and $j = 2$ the piezoelectric ceramics.

The partial differential equation of motion for both the polymers and piezoelectric ceramics is given by

$$\sigma_{rs,s} = \rho \ddot{u}_r, \quad D_{r,r} = 0, \tag{2}$$

where the summation convention is employed and dot denotes differentiation with respect to time, ρ the mass density of the polymers or piezoelectric ceramics, $r, s = 1, 3$ for the case of plane strain and here we will allow the subscripts x and z in Eq. (1) to be synonymous with 1 and 3 in Eq. (2). Substituting Eq. (1) into Eq. (2) leads to the following equations of wave motion:

$$c_{11}^{(j)} \frac{\partial^2 u_{xj}}{\partial x_j^2} + c_{44}^{(j)} \frac{\partial^2 u_{xj}}{\partial z_j^2} + \left[c_{13}^{(j)} + c_{44}^{(j)}\right] \frac{\partial^2 u_{zj}}{\partial x_j \partial z_j} + \left[e_{13}^{(j)} + e_{15}^{(j)}\right] \frac{\partial^2 \varphi_j}{\partial x_j \partial z_j} = \rho_j \frac{\partial^2 u_{xj}}{\partial t^2}, \tag{3a}$$

$$\left[c_{13}^{(j)} + c_{44}^{(j)}\right] \frac{\partial^2 u_{xj}}{\partial x_j \partial z_j} + c_{44}^{(j)} \frac{\partial^2 u_{zj}}{\partial x_j^2} + c_{33}^{(j)} \frac{\partial^2 u_{zj}}{\partial z_j^2} + e_{15}^{(j)} \frac{\partial^2 \varphi_j}{\partial x_j^2} + e_{33}^{(j)} \frac{\partial^2 \varphi_j}{\partial z_j^2} = \rho_j \frac{\partial^2 u_{zj}}{\partial t^2}, \tag{3b}$$

$$\left[e_{13}^{(j)} + e_{15}^{(j)}\right] \frac{\partial^2 u_{xj}}{\partial x_j \partial z_j} + e_{15}^{(j)} \frac{\partial^2 u_{zj}}{\partial x_j^2} + e_{33}^{(j)} \frac{\partial^2 u_{zj}}{\partial z_j^2} - \varepsilon_{11}^{(j)} \frac{\partial^2 \varphi_j}{\partial x_j^2} - \varepsilon_{33}^{(j)} \frac{\partial^2 \varphi_j}{\partial z_j^2} = 0. \tag{3c}$$

When P-waves or plane SV-waves polarized in the x direction propagate along the positive z direction, the displacements and electrical potential functions can be simplified and expressed as the following forms:

$$u_{xj}(z_j, t) = U_{xj}(z_j) \exp(-\mathrm{i}\omega t), \tag{4a}$$

$$u_{zj}(z_j, t) = U_{zj}(z_j) \exp(-\mathrm{i}\omega t), \tag{4b}$$

$$\varphi_j(z_j, t) = \Phi_j(z_j) \exp(-\mathrm{i}\omega t) \quad (j = 1, 2), \tag{4c}$$

where $i = \sqrt{-1}$, ω is the circular frequency, and $U_{xj}(z_j)$, $U_{zj}(z_j)$ and $\Phi_j(z_j)$ are the amplitudes of the displacements and electrical potential functions. Substituting Eqs. (4a)–(4c) into Eqs. (3a)–(3c) yields

$$c_{44}^{(j)} \frac{\mathrm{d}^2 U_{xj}}{\mathrm{d}z_j^2} + \rho_j \omega^2 U_{xj} = 0, \tag{5a}$$

$$c_{33}^{(j)} \frac{\mathrm{d}^2 U_{zj}}{\mathrm{d}z_j^2} + e_{33}^{(j)} \frac{\mathrm{d}^2 \Phi_j}{\mathrm{d}z_j^2} + \rho_j \omega^2 U_{zj} = 0, \tag{5b}$$

$$e_{33}^{(j)} \frac{\mathrm{d}^2 U_{zj}}{\mathrm{d}z_j^2} - \varepsilon_{33}^{(j)} \frac{\mathrm{d}^2 \Phi_j}{\mathrm{d}z_j^2} = 0, \tag{5c}$$

which can be converted into the following form:

$$\frac{\mathrm{d}^2 U_{xj}}{\mathrm{d}z_j^2} + k_{1j}^2 U_{xj} = 0, \tag{6a}$$

$$\frac{d^2U_{zj}}{dz_j^2} + k_{2j}^2 U_{zj} = 0, \tag{6b}$$

$$\frac{d^2\Phi_j}{dz_j^2} = p_j \frac{d^2U_{zj}}{dz_j^2}, \tag{6c}$$

where $p_j = e_{33}^{(j)}/\varepsilon_{33}^{(j)}$ is the ratio of the piezoelectric constant to the dielectric constant, $k_{1j} = \omega/c_{1j}$ and $k_{2j} = \omega/c_{2j}$ the wavenumbers, $c_{1j} = \sqrt{c_{44}^{(j)}/\rho_j}$ and $c_{2j} = \sqrt{\left[c_{33}^{(j)} + p_j e_{33}^{(j)}\right]/\rho_j}$ the phase velocities of the bulk waves in the polymers and the piezoelectric ceramics.

From Eqs. (6a)–(6c) we can see that U_{xj} is uncoupled from U_{zj} and Φ_j. And the general solutions of $U_{xj}(z_j)$, $U_{zj}(z_j)$ and $\Phi_j(z_j)$ can be written as

$$U_{xj}(z_j) = A_j \exp(-ik_{1j}z_j) + B_j \exp(ik_{1j}z_j), \tag{7a}$$

$$U_{zj}(z_j) = C_j \exp(-ik_{2j}z_j) + D_j \exp(ik_{2j}z_j), \tag{7b}$$

$$\Phi_j(z_j) = E_j + F_j z_j + p_j[C_j \exp(-ik_{2j}z_j) + D_j \exp(ik_{2j}z_j)] \quad (j = 1, 2), \tag{7c}$$

where A_j, B_j, C_j, D_j, E_j and F_j are the unknown coefficients.

3. Transfer matrix

In the following developments, we will introduce non-dimensional local coordinates of the polymeric and piezoelectric films, which may be convenient and simplifies the analytical process in the numerical simulations. The following dimensionless local coordinates are introduced

$$\xi_j = \frac{z_j}{\bar{a}_1} \quad (0 \leqslant \xi_j \leqslant \zeta_j) \quad (j = 1, 2), \tag{8}$$

where $\bar{a}_1$ is mean value of the thickness of the polymers and $\zeta_j = a_j/\bar{a}_1$ $(j = 1,2)$ are the dimensionless thickness of the polymers and the piezoelectric ceramics.

Suppose that the periodic piezoelectric composite structure as shown in Fig. 1 consists of $n+1$ unit cells. The ith unit cell is also displayed in Fig. 1. Every unit cell includes two sub-cells (sub-cell 1 and sub-cell 2), namely, the polymeric and piezoelectric thin films. The boundary conditions at the left and right sides of the two sub-cells in the ith unit cell are written by

$$u_{xjL}^{(i)} = u_{xj}^{(i)}\Big|_{z_j=0}, \quad u_{xjR}^{(i)} = u_{xj}^{(i)}\Big|_{z_j=a_j},$$

$$u_{zjL}^{(i)} = u_{zj}^{(i)}\Big|_{z_j=0}, \quad u_{zjR}^{(i)} = u_{zj}^{(i)}\Big|_{z_j=a_j},$$

$$\sigma_{xxjL}^{(i)} = \left[c_{11}^{(j)}\frac{\partial u_{xj}^{(i)}}{\partial x_j} + c_{13}^{(j)}\frac{\partial u_{zj}^{(i)}}{\partial z_j} + e_{13}^{(j)}\frac{\partial \varphi_j^{(i)}}{\partial z_j}\right]\Bigg|_{z_j=0}, \quad \sigma_{xxjR}^{(i)} = \left[c_{11}^{(j)}\frac{\partial u_{xj}^{(i)}}{\partial x_j} + c_{13}^{(j)}\frac{\partial u_{zj}^{(i)}}{\partial z_j} + e_{13}^{(j)}\frac{\partial \varphi_j^{(i)}}{\partial z_j}\right]\Bigg|_{z_j=a_j},$$

$$\sigma_{zzjL}^{(i)} = \left[c_{13}^{(j)}\frac{\partial u_{xj}^{(i)}}{\partial x_j} + c_{33}^{(j)}\frac{\partial u_{zj}^{(i)}}{\partial z_j} + e_{33}^{(j)}\frac{\partial \varphi_j^{(i)}}{\partial z_j}\right]\Bigg|_{z_j=0}, \quad \sigma_{zzjR}^{(i)} = \left[c_{13}^{(j)}\frac{\partial u_{xj}^{(i)}}{\partial x_j} + c_{33}^{(j)}\frac{\partial u_{zj}^{(i)}}{\partial z_j} + e_{33}^{(j)}\frac{\partial \varphi_j^{(i)}}{\partial z_j}\right]\Bigg|_{z_j=a_j},$$

$$\sigma_{xzjL}^{(i)} = \left[c_{44}^{(j)}\frac{\partial u_{xj}^{(i)}}{\partial z_j} + c_{44}^{(j)}\frac{\partial u_{zj}^{(i)}}{\partial x_j} + e_{15}^{(j)}\frac{\partial \varphi_j^{(i)}}{\partial x_j}\right]\Bigg|_{z_j=0}, \quad \sigma_{xzjR}^{(i)} = \left[c_{44}^{(j)}\frac{\partial u_{xj}^{(i)}}{\partial z_j} + c_{44}^{(j)}\frac{\partial u_{zj}^{(i)}}{\partial x_j} + e_{15}^{(j)}\frac{\partial \varphi_j^{(i)}}{\partial x_j}\right]\Bigg|_{z_j=a_j},$$

$$\varphi_{jL}^{(i)} = \varphi_j^{(i)}\Big|_{z_j=0}, \quad \varphi_{jR}^{(i)} = \varphi_j^{(i)}\Big|_{z_j=a_j},$$

$$D_{xjL}^{(i)} = \left[e_{15}^{(j)}\frac{\partial u_{xj}^{(i)}}{\partial z_j} + e_{15}^{(j)}\frac{\partial u_{zj}^{(i)}}{\partial x_j} - \varepsilon_{11}^{(j)}\frac{\partial \varphi_j^{(i)}}{\partial x_j}\right]\Bigg|_{z_j=0}, \quad D_{xjR}^{(i)} = \left[e_{15}^{(j)}\frac{\partial u_{xj}^{(i)}}{\partial z_j} + e_{15}^{(j)}\frac{\partial u_{zj}^{(i)}}{\partial x_j} - \varepsilon_{11}^{(j)}\frac{\partial \varphi_j^{(i)}}{\partial x_j}\right]\Bigg|_{z_j=a_j},$$

$$D_{zjL}^{(i)} = \left[e_{13}^{(j)}\frac{\partial u_{xj}^{(i)}}{\partial x_j} + e_{33}^{(j)}\frac{\partial u_{zj}^{(i)}}{\partial z_j} - \varepsilon_{33}^{(j)}\frac{\partial \varphi_j^{(i)}}{\partial z_j}\right]\Bigg|_{z_j=0}, \quad D_{zjR}^{(i)} = \left[e_{13}^{(j)}\frac{\partial u_{xj}^{(i)}}{\partial x_j} + e_{33}^{(j)}\frac{\partial u_{zj}^{(i)}}{\partial z_j} - \varepsilon_{33}^{(j)}\frac{\partial \varphi_j^{(i)}}{\partial z_j}\right]\Bigg|_{z_j=a_j},$$
$$(j = 1, 2;\ i = 1, 2, \ldots, n+1), \tag{9}$$

where the subscripts L and R denote the left and right sides of the two sub-cells in the ith unit cell.

Substituting Eqs. (1a)–(1e), (4a)–(4c), (7a)–(7c) and (8) into Eq. (9), one can get the following formulations:

$$\begin{cases} u_{xjL}^{(i)} = (A_j + B_j)\exp(-\mathrm{i}\omega t), \\ u_{xjR}^{(i)} = \left[A_j\exp(-\mathrm{i}\alpha_{1j}\zeta_j) + B_j\exp(\mathrm{i}\alpha_{1j}\zeta_j)\right]\exp(-\mathrm{i}\omega t), \end{cases} \tag{10a}$$

$$\begin{cases} u_{zjL}^{(i)} = (C_j + D_j)\exp(-\mathrm{i}\omega t), \\ u_{zjR}^{(i)} = \left[C_j\exp(-\mathrm{i}\alpha_{2j}\zeta_j) + D_j\exp(\mathrm{i}\alpha_{2j}\zeta_j)\right]\exp(-\mathrm{i}\omega t), \end{cases} \tag{10b}$$

$$\begin{cases} \sigma_{xxjL}^{(i)} = \left\{\frac{-\mathrm{i}C_j\alpha_{2j}+\mathrm{i}D_j\alpha_{2j}}{\tilde{a}_1}\left[c_{13}^{(j)} + p_j e_{13}^{(j)}\right] + F_j e_{13}^{(j)}\right\}\exp(-\mathrm{i}\omega t), \\ \sigma_{xxjR}^{(i)} = \left\{\frac{-\mathrm{i}C_j\alpha_{2j}\exp(-\mathrm{i}\alpha_{2j}\zeta_j)+\mathrm{i}D_j\alpha_{2j}\exp(\mathrm{i}\alpha_{2j}\zeta_j)}{\tilde{a}_1}\left[c_{13}^{(j)} + p_j e_{13}^{(j)}\right] + F_j e_{13}^{(j)}\right\}\exp(-\mathrm{i}\omega t), \end{cases} \tag{10c}$$

$$\begin{cases} \sigma_{zzjL}^{(i)} = \left\{\frac{-\mathrm{i}C_j\alpha_{2j}+\mathrm{i}D_j\alpha_{2j}}{\tilde{a}_1}\left[c_{33}^{(j)} + p_j e_{33}^{(j)}\right] + F_j e_{33}^{(j)}\right\}\exp(-\mathrm{i}\omega t), \\ \sigma_{zzjR}^{(i)} = \left\{\frac{-\mathrm{i}C_j\alpha_{2j}\exp(-\mathrm{i}\alpha_{2j}\zeta_j)+\mathrm{i}D_j\alpha_{2j}\exp(\mathrm{i}\alpha_{2j}\zeta_j)}{\tilde{a}_1}\left[c_{33}^{(j)} + p_j e_{33}^{(j)}\right] + F_j e_{33}^{(j)}\right\}\exp(-\mathrm{i}\omega t), \end{cases} \tag{10d}$$

$$\begin{cases} \sigma_{xzjL}^{(i)} = \frac{c_{44}^{(j)}(-\mathrm{i}A_j\alpha_{1j}+\mathrm{i}B_j\alpha_{1j})}{\tilde{a}_1}\exp(-\mathrm{i}\omega t), \\ \sigma_{xzjR}^{(i)} = \frac{c_{44}^{(j)}\left[-\mathrm{i}A_j\alpha_{1j}\exp(-\mathrm{i}\alpha_{1j}\zeta_j)+\mathrm{i}B_j\alpha_{1j}\exp(\mathrm{i}\alpha_{1j}\zeta_j)\right]}{\tilde{a}_1}\exp(-\mathrm{i}\omega t), \end{cases} \tag{10e}$$

$$\begin{cases} \varphi_{jL}^{(i)} = \left[E_j + p_j(C_j + D_j)\right]exp(-\mathrm{i}\omega t), \\ \varphi_{jR}^{(i)} = \left\{E_j + F_j\tilde{a}_1\zeta_j + p_j\left[C_j\exp(-\mathrm{i}\alpha_{2j}\zeta_j) + D_j\exp(i\alpha_{2j}\zeta_j)\right]\right\}\exp(-\mathrm{i}\omega t), \end{cases} \tag{10f}$$

$$\begin{cases} D_{xjL}^{(i)} = \frac{e_{15}^{(j)}(-\mathrm{i}A_j\alpha_{1j}+\mathrm{i}B_j\alpha_{1j})}{\tilde{a}_1}\exp(-\mathrm{i}\omega t), \\ D_{xjR}^{(i)} = \frac{e_{15}^{(j)}\left[-\mathrm{i}A_j\alpha_{1j}\exp(-\mathrm{i}\alpha_{1j}\zeta_j)+\mathrm{i}B_j\alpha_{1j}\exp(\mathrm{i}\alpha_{1j}\zeta_j)\right]}{\tilde{a}_1}\exp(-\mathrm{i}\omega t), \end{cases} \tag{10g}$$

$$\begin{cases} D_{zjL}^{(i)} = -F_j\varepsilon_{33}^{(j)}\exp(-\mathrm{i}\omega t), \\ D_{zjR}^{(i)} = -F_j\varepsilon_{33}^{(j)}\exp(-\mathrm{i}\omega t), \end{cases} \tag{10h}$$

where $\alpha_{1j} = k_{1j}\tilde{a}_1$ and $\alpha_{2j} = k_{2j}\tilde{a}_1$ are the non-dimensional wavenumbers.

It can be seen from Eqs. (10c)–(10e), (10g) and (10h), that their both sides can be non-dimensionalized if we define the following non-dimensional variables:

$$\tilde{\sigma}^{(i)}_{xxjR}=\frac{\bar{a}_1\sigma^{(i)}_{xxjR}}{c^{(j)}_{13}},\quad \tilde{\sigma}^{(i)}_{zzjR}=\frac{\bar{a}_1\sigma^{(i)}_{zzjR}}{c^{(j)}_{33}},\quad \tilde{\sigma}^{(i)}_{xzjR}=\frac{\bar{a}_1\sigma^{(i)}_{xzjR}}{c^{(j)}_{44}},\quad \tilde{D}^{(i)}_{xjR}=\frac{\bar{a}_1D^{(i)}_{xjR}}{e^{(j)}_{15}},\quad \tilde{D}^{(i)}_{zjR}=\frac{\bar{a}_1D^{(i)}_{zjR}}{e^{(j)}_{33}},\tag{11a}$$

$$\tilde{\sigma}^{(i)}_{xxjL}=\frac{\bar{a}_1\sigma^{(i)}_{xxjL}}{c^{(j)}_{13}},\quad \tilde{\sigma}^{(i)}_{zzjL}=\frac{\bar{a}_1\sigma^{(i)}_{zzjL}}{c^{(j)}_{33}},\quad \tilde{\sigma}^{(i)}_{xzjL}=\frac{\bar{a}_1\sigma^{(i)}_{xzjL}}{c^{(j)}_{44}},\quad \tilde{D}^{(i)}_{xjL}=\frac{\bar{a}_1D^{(i)}_{xjL}}{e^{(j)}_{15}},\quad \tilde{D}^{(i)}_{zjL}=\frac{\bar{a}_1D^{(i)}_{zjL}}{e^{(j)}_{33}},\tag{11b}$$

Then Eqs. (10c)–(10e), (10g) and (10h), can be transformed into the following dimensionless forms:

$$\begin{cases}\tilde{\sigma}^{(i)}_{xxjL}=\left\{(-\mathrm{i}C_j\alpha_{2j}+\mathrm{i}D_j\alpha_{2j})\left[1+p_je^{(j)}_{13}/c^{(j)}_{13}\right]+F_j\bar{a}_1e^{(j)}_{13}/c^{(j)}_{13}\right\}\exp(-\mathrm{i}\omega t),\\ \tilde{\sigma}^{(i)}_{xxjR}=\left\{\left[-\mathrm{i}C_j\alpha_{2j}\exp(-\mathrm{i}\alpha_{2j}\zeta_j)+\mathrm{i}D_j\alpha_{2j}\exp(\mathrm{i}\alpha_{2j}\zeta_j)\right]\left[1+p_je^{(j)}_{13}/c^{(j)}_{13}\right]+F_j\bar{a}_1e^{(j)}_{13}/c^{(j)}_{13}\right\}\exp(-\mathrm{i}\omega t),\end{cases}\tag{12a}$$

$$\begin{cases}\tilde{\sigma}^{(i)}_{zzjL}=\left\{(-\mathrm{i}C_j\alpha_{2j}+\mathrm{i}D_j\alpha_{2j})\left[1+p_je^{(j)}_{33}/c^{(j)}_{33}\right]+F_j\bar{a}_1e^{(j)}_{33}/c^{(j)}_{33}\right\}\exp(-\mathrm{i}\omega t),\\ \tilde{\sigma}^{(i)}_{zzjR}=\left\{\left[-\mathrm{i}C_j\alpha_{2j}\exp(-\mathrm{i}\alpha_{2j}\zeta_j)+\mathrm{i}D_j\alpha_{2j}\exp(\mathrm{i}\alpha_{2j}\zeta_j)\right]\left[1+p_je^{(j)}_{33}/c^{(j)}_{33}\right]+F_j\bar{a}_1e^{(j)}_{33}/c^{(j)}_{33}\right\}\exp(-\mathrm{i}\omega t),\end{cases}\tag{12b}$$

$$\begin{cases}\tilde{\sigma}^{(i)}_{xzjL}=(-\mathrm{i}A_j\alpha_{1j}+\mathrm{i}B_j\alpha_{1j})\exp(-\mathrm{i}\omega t),\\ \tilde{\sigma}^{(i)}_{xzjR}=\left[-\mathrm{i}A_j\alpha_{1j}\exp(-\mathrm{i}\alpha_{1j}\zeta_j)+\mathrm{i}B_j\alpha_{1j}\exp(\mathrm{i}\alpha_{1j}\zeta_j)\right]\exp(-\mathrm{i}\omega t),\end{cases}\tag{12c}$$

$$\begin{cases}\tilde{D}^{(i)}_{xjL}=(-\mathrm{i}A_j\alpha_{1j}+\mathrm{i}B_j\alpha_{1j})\exp(-\mathrm{i}\omega t),\\ \tilde{D}^{(i)}_{xjR}=\left[-\mathrm{i}A_j\alpha_{1j}\exp(-\mathrm{i}\alpha_{1j}\zeta_j)+\mathrm{i}B_j\alpha_{1j}\exp(\mathrm{i}\alpha_{1j}\zeta_j)\right]\exp(-\mathrm{i}\omega t),\end{cases}\tag{12d}$$

$$\begin{cases}\tilde{D}^{(i)}_{zjL}=\left[-F_j\bar{a}_1\varepsilon^{(j)}_{33}/e^{(j)}_{33}\right]\exp(-\mathrm{i}\omega t),\\ \tilde{D}^{(i)}_{zjR}=\left[-F_j\bar{a}_1\varepsilon^{(j)}_{33}/e^{(j)}_{33}\right]\exp(-\mathrm{i}\omega t).\end{cases}\tag{12e}$$

We can observe that the right sides of Eqs. (12c) and (12d) are equal to each other. So only one of them is necessary to be considered. Moreover, it is observed from Eq. (12e) that the amplitude values of the non-dimensional electric displacements $\tilde{D}^{(i)}_{zjR}$ and $\tilde{D}^{(i)}_{zjL}$ at the right and left sides of the two sub-cells are equal to each other, i.e. the amplitude values of the waves corresponding to the electric displacement $D^{(i)}_{zj}$ do not attenuate along the piezoelectric composite structures. So it is not necessary to study the localization problem about the waves corresponding to the electric displacement $D^{(i)}_{zj}$. Due to the above reasons, Eqs. (12d) and (12e) will be omitted during the following studies.

Eqs. (10a), (10b), (10f) and (12a)–(12c), are chosen to calculate the relational expression between the right and left sides of the ith unit cell. Eliminating the unknown coefficients A_j, B_j, C_j, D_j, E_j and $\bar{a}_1F_j$ from these six chosen equations and solving for $u^{(i)}_{xjR}$, $\tilde{\sigma}^{(i)}_{xzjR}$, $u^{(i)}_{zjR}$, $\tilde{\sigma}^{(i)}_{xxjR}$, $\tilde{\sigma}^{(i)}_{zzjR}$ and $\varphi^{(i)}_{jR}$ in terms of $u^{(i)}_{xjL}$, $\tilde{\sigma}^{(i)}_{xzjL}$, $u^{(i)}_{zjL}$, $\tilde{\sigma}^{(i)}_{xxjL}$, $\tilde{\sigma}^{(i)}_{zzjL}$ and $\varphi^{(i)}_{jL}$ results in the following matrix equation:

$$\mathbf{v}^{(i)}_{jR}=\mathbf{T}'_j\mathbf{v}^{(i)}_{jL},\quad (j=1,2;\ \ i=1,2,\ldots,n+1),\tag{13}$$

where $\mathbf{T}'_j$ is the transfer matrix of the two sub-cells. And the elements of $\mathbf{T}'_j$ are dimensionless and are given in Appendix A. $\mathbf{v}^{(i)}_{jR}$ and $\mathbf{v}^{(i)}_{jL}$ are the state vectors at right and left sides of the two sub-cells and are written as

$$\begin{aligned}\mathbf{v}^{(i)}_{jR}&=\left\{u^{(i)}_{xjR},\tilde{\sigma}^{(i)}_{xzjR},u^{(i)}_{zjR},\tilde{\sigma}^{(i)}_{xxjR},\tilde{\sigma}^{(i)}_{zzjR},\varphi^{(i)}_{jR}\right\}^{\mathrm{T}},\\ \mathbf{v}^{(i)}_{jL}&=\left\{u^{(i)}_{xjL},\tilde{\sigma}^{(i)}_{xzjL},u^{(i)}_{zjL},\tilde{\sigma}^{(i)}_{xxjL},\tilde{\sigma}^{(i)}_{zzjL},\varphi^{(i)}_{jL}\right\}^{\mathrm{T}}.\end{aligned}\tag{14}$$

The following condition is satisfied at the interface between the two sub-cells

$$\mathbf{v}_{1R}^{(i)} = \mathbf{v}_{2L}^{(i)}. \tag{15}$$

Thus the relationship between the right and left sides of the ith unit cell can be obtained from Eq. (13) as

$$\mathbf{v}_{2R}^{(i)} = \mathbf{T}_i \mathbf{v}_{1L}^{(i)} \quad (i = 2, \ldots, n+1). \tag{16}$$

where $\mathbf{T}_i$ is the transfer matrix of the ith unit cell and is given by

$$\mathbf{T}_i = \mathbf{T}_2' \mathbf{T}_1' \tag{17}$$

At the interface between the right side of the $(i-1)$th unit cell and the left side of the ith unit cell, the following condition is satisfied:

$$\mathbf{v}_{1L}^{(i)} = \mathbf{v}_{2R}^{(i-1)} \quad (i = 2, \ldots, n+1). \tag{18}$$

Substituting Eq. (18) into Eq. (16), one can obtain the following relation between the state vectors of the $(i-1)$th and the ith unit cells

$$\mathbf{v}_{2R}^{(i)} = \mathbf{T}_i \mathbf{v}_{2R}^{(i-1)} \quad (i = 2, \ldots, n+1), \tag{19}$$

from which one can observe that $\mathbf{T}_i$ is the transfer matrix between two consecutive unit cells.

4. Wave localization factor

Lyapunov exponent measures the average exponential rate of convergence or divergence between two neighboring phase orbits in phase space. Employing the concept of Lyapunov exponent, one can get a measurable index about the rate of decay of wave amplitudes during studying wave localization in disordered periodic structures. According to the symmetry of periodic structures, it can be proved that Lyapunov exponents always occur in pairs, i.e. if λ is a Lyapunov exponent then $-\lambda$ is also a Lyapunov exponent [9]. Therefore, for $2m \times 2m$ transfer matrices, the m pairs of Lyapunov exponents have the following property, $\lambda_1 \geqslant \lambda_2 \geqslant \cdots \geqslant \lambda_m \geqslant 0 \geqslant \lambda_{m+1}(=-\lambda_m) \geqslant \lambda_{m+2}(=-\lambda_{m-1}) \geqslant \cdots \geqslant \lambda_{2m}(=-\lambda_1)$. Localization factor which is defined by the smallest positive Lyapunov λ_m is used to characterize the average exponential rate of decay of wave amplitudes. Since λ_m represents the wave that has the least amount of decay and transmits energy farther along the structure than any other waves. So, it characterizes the main decay behavior of elastic waves.

In the present work, the algorithm for calculating Lyapunov exponents in continuous dynamical systems by Wolf et al. [13] is applied to calculate the Lyapunov exponents in the discrete dynamical system, Eq. (19). The formulation for calculating the mth, $1 \leqslant m \leqslant 2d$, Lyapunov exponent is written as follows:

$$\lambda_m = \lim_{n\to\infty} \frac{1}{n} \sum_{i=1}^{n} \ln \left\| \hat{\mathbf{v}}_{2R,m}^{(i+1)} \right\|, \tag{20}$$

where the vector $\hat{\mathbf{v}}_{2R,m}^{(i+1)}$ will be defined in what follows. To calculate the mth Lyapunov exponent $(1 \leqslant m \leqslant 2d)$, m orthogonal unit vectors of $2d$-dimension, $\mathbf{u}_1^{(1)}, \mathbf{u}_2^{(1)}, \cdots, \mathbf{u}_m^{(1)}$, are chosen as the initial state vectors. Then Eq. (19) is used to compute the state vectors iteratively. At the ith iteration

$$\hat{\mathbf{v}}_{2R,k}^{(i+1)} = \mathbf{T}_{i+1} \mathbf{u}_k^{(i)} \quad (i = 1, 2, \ldots n;\ k = 1, 2, \ldots, m), \tag{21}$$

where the vectors $\mathbf{u}_k^{(i)}$ are unit and orthogonal, while the vectors $\mathbf{v}_{2R,k}^{(i+1)}$ $(k = 1, 2, \ldots, m)$ are usually not orthogonal. The Gram–Schmidt orthonormalization procedure is now applied to produce m orthogonal unit vectors

$$\hat{\mathbf{v}}_{2R,1}^{(i+1)} = \mathbf{v}_{2R,1}^{(i+1)}, \quad \mathbf{u}_1^{(i+1)} = \frac{\hat{\mathbf{v}}_{2R,1}^{(i+1)}}{\left\| \hat{\mathbf{v}}_{2R,1}^{(i+1)} \right\|},$$

$$\hat{\mathbf{v}}_{2R,2}^{(i+1)} = \hat{\mathbf{v}}_{2R,2}^{(i+1)} - (\hat{\mathbf{v}}_{2R,2}^{(i+1)}, \mathbf{u}_1^{(i+1)})\mathbf{u}_1^{(i+1)}, \quad \mathbf{u}_2^{(i+1)} = \frac{\hat{\mathbf{v}}_{2R,2}^{(i+1)}}{\left\|\hat{\mathbf{v}}_{2R,2}^{(i+1)}\right\|},$$

$$\vdots$$

$$\hat{\mathbf{v}}_{2R,m}^{(i+1)} = \mathbf{v}_{2R,m}^{(i+1)} - (\mathbf{v}_{2R,m}^{(i+1)}, \mathbf{u}_{m-1}^{(i+1)})\mathbf{u}_{m-1}^{(i+1)} - \cdots - (\mathbf{v}_{2R,m}^{(i+1)}, \mathbf{u}_1^{(i+1)})\mathbf{u}_1^{(i+1)}, \quad \mathbf{u}_m^{(i+1)} = \frac{\hat{\mathbf{v}}_{2R,m}^{(i+1)}}{\left\|\hat{\mathbf{v}}_{2R,m}^{(i+1)}\right\|}, \tag{22}$$

where $(\cdot,\cdot)$ denotes the dot-product. By means of Eq. (20), each of the m pairs of contrary Lyapunov exponents can be calculated. The mth Lyapunov exponent λ_m is the localization factor. Then it is implied that the wave amplitudes decay at the magnitude $\exp(-\lambda_m)$ when they propagate through each unit cell.

5. Example and discussions

In this section, numerical simulation for randomly disordered periodic layered piezoelectric composite structures is performed to study the characters of propagation and localization of plane elastic waves with different frequencies. The non-dimensional thickness of the polymers, ζ_1, is assumed to be uniformly distributed random variable with mean value, $\bar{\zeta}_1$, and coefficient of variance, δ. So ζ_1 is a random number distributed in the interval $\left[\bar{\zeta}_1(1-\sqrt{3}\delta), \bar{\zeta}_1(1+\sqrt{3}\delta)\right]$. Hence, if z is a standard uniformly distributed random variable, i.e. $z \in (0,1)$, then ζ_1 can be expressed as the following formulation

$$\zeta_1 = \bar{\zeta}_1\left[1 + \sqrt{3}\delta(2z-1)\right]. \tag{23}$$

The material constants of the polymers and piezoelectric ceramics are from Refs. [12,14,15] and listed in Table 1.

The localization factors for disordered periodic layered piezoelectric composite structures are determined using Eq. (20). For the ith iteration, a random number z is generated for the non-dimensional thickness of the polymers and the elements of the transfer matrices are calculated. Three values of the coefficient of variation of the dimensionless thickness ζ_1, i.e. $\delta = 0$, 0.05 and 0.1 are considered. The case of $\delta = 0$ corresponds to the perfectly periodic structures.

For three kinds of disordered periodic piezoelectric composite structures, i.e. PVDF-PZT-2, PVDF-PZT-4 and PVDF-PZT-5H piezocomposites, Figs. 2–4 display the variations of the localization factors versus non-dimensional wavenumber α_{11} for $\delta = 0$, 0.05 and 0.1. It can be observed from these figures that ordered periodic structures ($\delta = 0$) have the properties of frequency passbands and stopbands, and a localization phenomenon can occur in disordered periodic structures. For example, as seen in Fig. 2 by the solid line, the interval $\alpha_{11} \in (2.6, 3.45)$ in which the localization factors are zero is called the passband and the interval $\alpha_{11} \in (3.45, 4.6)$ is known as the stopband for the localization factors are bigger than zero at this frequency

Table 1
Material constants of the polymers and piezoceramics

Materials	Mass density (10^3 kg/m^3)	Elastic constants (10^{10} N/m^2)			Piezoelectric constant (C/m^2)			Dielectric constants (10^{-10} F/m)
	ρ	c_{13}	c_{33}	c_{44}	e_{13}	e_{15}	e_{33}	ε_{33}
Polymer								
PVDF	1.78	1.0	1.2	0.7	0.024	0.0	−0.027	0.6726
Piezoceramics								
PZT-2	7.60	6.81	11.3	2.22	−1.90	9.80	9.00	23.02
PZT-4	7.50	7.43	11.3	2.56	−6.98	12.7	13.8	54.70
PZT-5H	7.50	8.41	11.7	2.30	−6.50	17.0	23.3	130.0

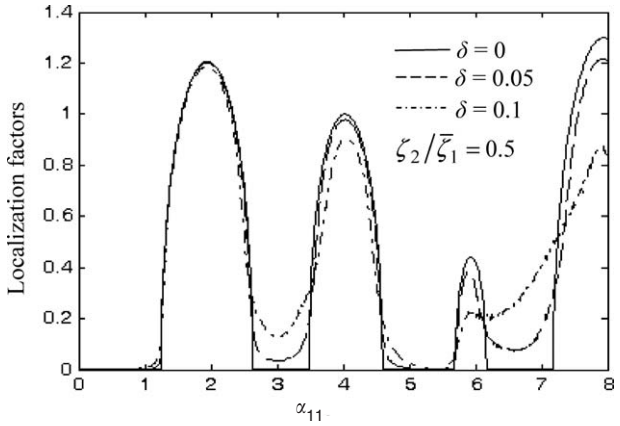

Fig. 2. Localization factors versus non-dimensional wavenumber α_{11} for disordered periodic PVDF-PZT-2 piezocomposites.

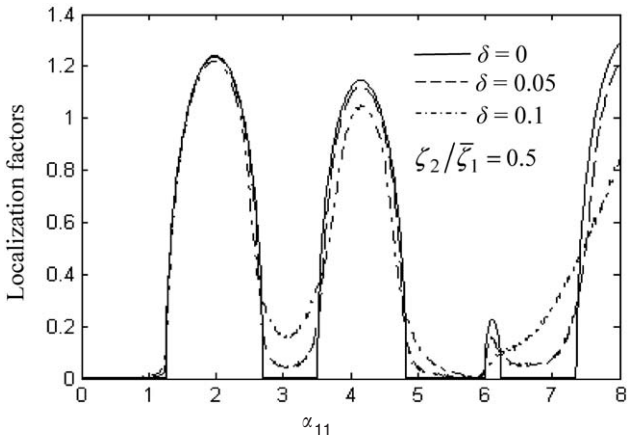

Fig. 3. Localization factors versus non-dimensional wavenumber α_{11} for disordered periodic PVDF-PZT-4 piezocomposites.

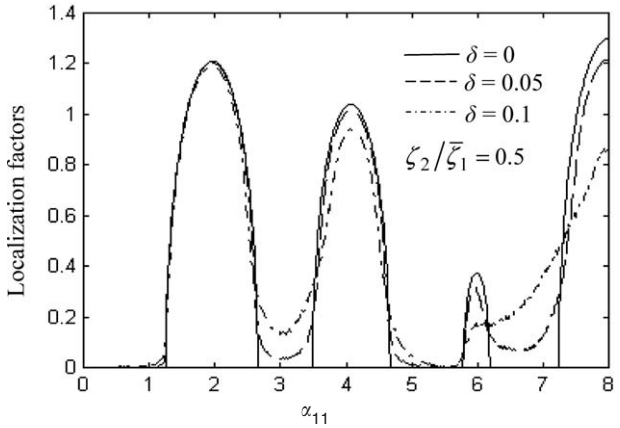

Fig. 4. Localization factors versus non-dimensional wavenumber α_{11} for disordered periodic PVDF-PZT-5H piezocomposites.

region. However, we can see that for disordered periodic structures the localization factors are not zero but positive in the frequency passbands of the corresponding tuned periodic structures, which means that the phenomenon of wave localization occurs. Moreover, with the increase of the coefficient of variation δ, the magnitudes of the localization factors in passbands are also increased and consequently the degree of wave localization is strengthened.

It can also be seen from Figs. 2–4 that for different disordered periodic piezocomposites the characters of wave localization have some changes. In these three figures, the characters of the third stopbands (near $\alpha_{11} = 6.0$) are more different between Figs. 2 and 3 and Figs. 3 and 4. But there are little differences between Figs. 2 and 4. We can also see from these three figures that in the first passband of the corresponding ordered periodic structures the degrees of wave localization in disordered periodic ones are very weak even for lager coefficient of variation δ (e.g. $\delta = 0.1$), but in the second and fourth passbands the degrees of wave localization in disordered periodic structures are strong even for smaller δ (e.g. $\delta = 0.05$).

For two kinds of disordered periodic piezocomposites, i.e. PVDF-PZT-4 and PVDF-PZT-5H, Figs. 5 and 6 show the variations of the localization factors versus the ratio of the non-dimensional thickness ζ_2 of the piezoelectric ceramics to the mean value ζ_1 of the non-dimensional thickness of the polymers for $\alpha_{11} = 2.0$ and 3.0. From Figs. 5 and 6 we can observe some interesting phenomena. For example, for ordered periodic structures, the intervals of passbands and stopbands periodically appear with the increase of the ratio $\zeta_2/\bar{\zeta}_1$. For the case of $\alpha_{11} = 2.0$, weak localization phenomena occur as the localization factors are close to zero in larger regions of the passbands for the disordered periodic structures. But for the case of $\alpha_{11} = 3.0$, strong localization phenomena appear as the localization factors are bigger than zero in the passbands regions except for some points when $\delta > 0$.

It can be seen from Figs. 5(a) and 5(b) or 6(a) and 6(b) that for $\alpha_{11} = 2.0$ the width of the passbands is narrower than that of the stopbands for ordered periodic structures. But for $\alpha_{11} = 3.0$ the width of the stopbands is very narrow and that of the passbands is very broad. So we can adjust the ratio of the thickness of the piezoelectric ceramics to that of the polymers to control the characters of wave propagation. Moreover, it is observed from Figs. 5(a) and 6(a) or 5(b) and 6(b) that for different ordered periodic piezocomposites ($\delta = 0$) the locations of passbands or stopbands are also different. The passbands or stopbands of the

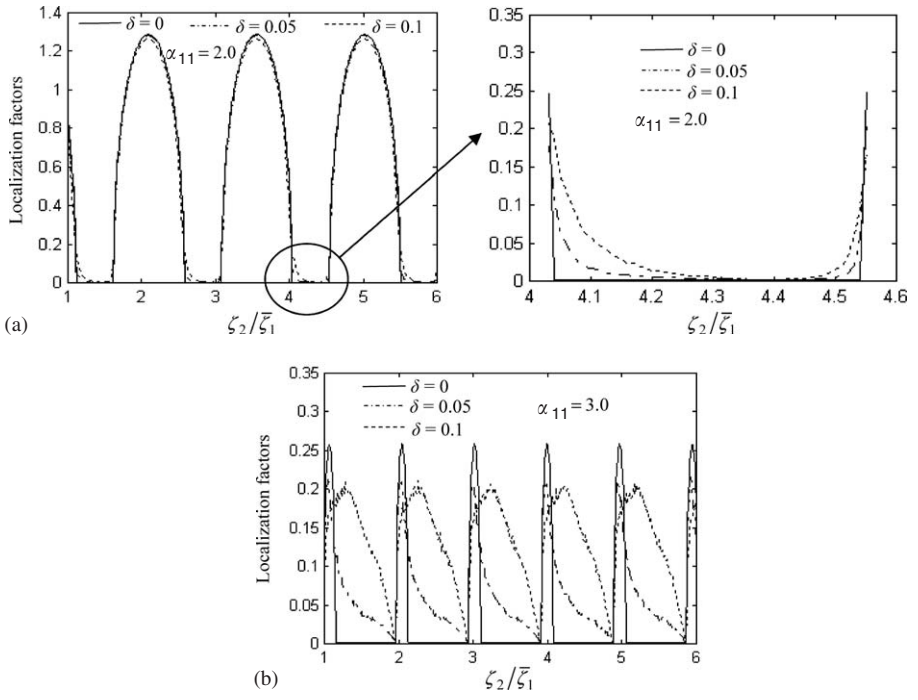

Fig. 5. Localization factors versus the ratio of $\zeta_2/\bar{\zeta}_1$ for disordered periodic PVDF-PZT-4 piezocomposites with the consideration of $\alpha_{11} = 2.0$ and 3.0.

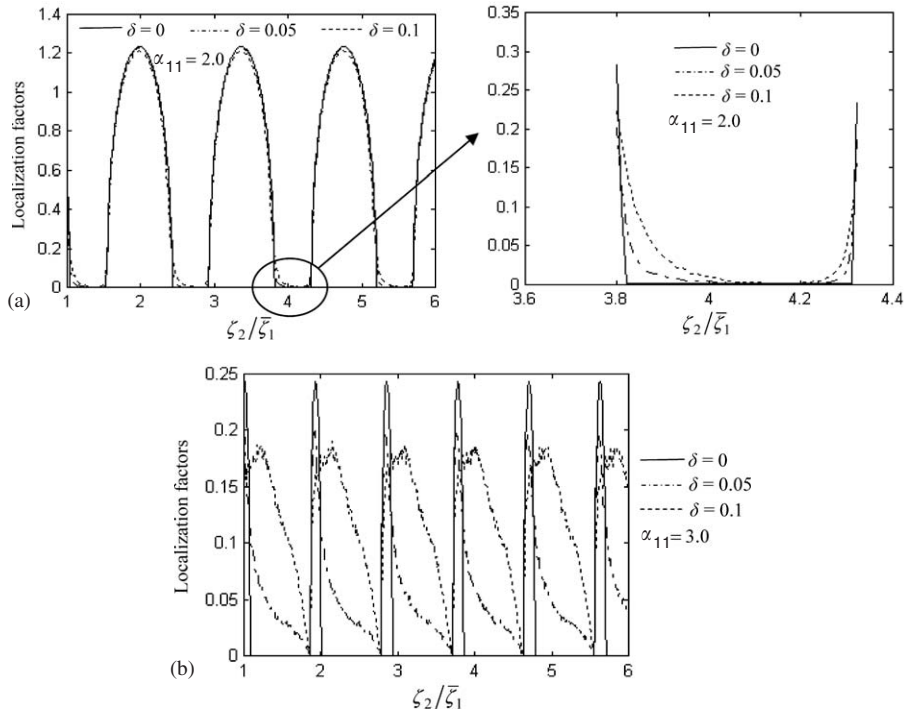

Fig. 6. Localization factors versus the ratio of $\zeta_2/\bar{\zeta}_1$ for disordered periodic PVDF-PZT-5H piezocomposites with the consideration of $\alpha_{11} = 2.0$ and 3.0.

PVDF-PZT-4 piezocomposites shift a little distance towards left compared with those of the PVDF-PZT-5H piezocomposites.

6. Conclusions

In the present work, wave propagation and localization in disordered periodic 2–2 piezoelectric composite structures are studied. The mechanical and electrical coupling characters of piezoelectric composite materials are considered. The transfer matrix between two consecutive unit cells is obtained and the expression of localization factor in disordered periodic structures is presented. As examples, numerical simulations of localization factors for three kinds of disordered periodic piezoelectric composite structures, i.e. PVDF-PZT-2, PVDF-PZT-4 and PVDF-PZT-5H piezocomposites are presented and discussed. From the results we can draw the following conclusions:

(1) The properties of frequency passbands and stopbands in ordered periodic structures and the phenomenon of wave localization in disordered periodic structures are observed, and the larger the coefficient of variation, the stronger the degree of wave localization.
(2) For one sort of piezocomposites the properties of wave propagation and localization are very different for different ratios of the thickness of the piezoelectric ceramics to that of the polymers, and even for the same ratios the characters of wave localization are also very different for different non-dimensional wavenumbers α_{11}.
(3) For different sorts of periodic piezocomposites the locations of passbands or stopbands are different for same non-dimensional wavenumbers α_{11}. We may design different piezocomposites or adjust the ratio of the thickness of the piezoelectric ceramics to that of the polymers to control the characters of wave propagation.

Acknowledgements

The authors wish to express gratitude for the support provided by the National Science Fund for Distinguished Young Scholars under grant no. 10025211. The first author is also grateful to the support by the NJTU Paper Foundation of China under grant no. PD250, the China Postdoctoral Science Foundation under grant no. 2004035269 and the Beijing Special Foundation for the Cultivation of Excellent Scholars under grant no. 20042D0500504 for this research work.

Appendix A

The elements of the transfer matrices of two sub-cells in the ith unit cell of disordered periodic 2–2 piezoelectric composite structures are written as

$$T'_j(1,1)=\frac{\exp(-\mathrm{i}\alpha_{1j}\zeta_j)+\exp(\mathrm{i}\alpha_{1j}\zeta_j)}{2},\quad T'_j(1,2)=\frac{-\mathrm{i}\left[-\exp(-\mathrm{i}\alpha_{1j}\zeta_j)+\exp(\mathrm{i}\alpha_{1j}\zeta_j)\right]}{2\alpha_{1j}},$$

$$T'_j(1,3)=T'_j(1,4)=T'_j(1,5)=T'_j(1,6)=0,$$

$$T'_j(2,1)=\frac{\mathrm{i}\alpha_{1j}\left[-\exp(-\mathrm{i}\alpha_{1j}\zeta_j)+\exp(\mathrm{i}\alpha_{1j}\zeta_j)\right]}{2},\quad T'_j(2,2)=\frac{\exp(-\mathrm{i}\alpha_{1j}\zeta_j)+\exp(\mathrm{i}\alpha_{1j}\zeta_j)}{2},$$

$$T'_j(2,3)=T'_j(2,4)=T'_j(2,5)=T'_j(2,6)=0,$$

$$T'_j(3,1)=T'_j(3,2)=0,\quad T'_j(3,3)=\frac{\exp(-\mathrm{i}\alpha_{2j}\zeta_j)+\exp(\mathrm{i}\alpha_{2j}\zeta_j)}{2},$$

$$T'_j(3,4)=\frac{-\mathrm{i}e_{33}^{(j)}\left[-\exp(-\mathrm{i}\alpha_{2j}\zeta_j)+\exp(\mathrm{i}\alpha_{2j}\zeta_j)\right]}{2\alpha_{2j}\left[-c_{33}^{(j)}e_{13}^{(j)}+c_{13}^{(j)}e_{33}^{(j)}\right]},$$

$$T'_j(3,5)=\frac{-\mathrm{i}e_{13}^{(j)}\left[-\exp(-\mathrm{i}\alpha_{2j}\zeta_j)+\exp(\mathrm{i}\alpha_{2j}\zeta_j)\right]}{2\alpha_{2j}\left[c_{33}^{(j)}e_{13}^{(j)}-c_{13}^{(j)}e_{33}^{(j)}\right]},\quad T'_j(3,6)=0,$$

$$T'_j(4,1)=T'_j(4,2)=0,\quad T'_j(4,3)=\frac{\mathrm{i}\alpha_{2j}\left[c_{13}^{(j)}+p_je_{13}^{(j)}\right]\left[-\exp(-\mathrm{i}\alpha_{2j}\zeta_j)+\exp(\mathrm{i}\alpha_{2j}\zeta_j)\right]}{2},$$

$$T'_j(4,4)=\frac{2c_{33}^{(j)}e_{13}^{(j)}-e_{33}^{(j)}\exp(-\mathrm{i}\alpha_{2j}\zeta_j)\left\{c_{13}^{(j)}\left[1+\exp(2\mathrm{i}\alpha_{2j}\zeta_j)\right]+p_je_{13}^{(j)}\left[-1+\exp(\mathrm{i}\alpha_{2j}\zeta_j)\right]^2\right\}}{2\left[c_{33}^{(j)}e_{13}^{(j)}-c_{13}^{(j)}e_{33}^{(j)}\right]},$$

$$T'_j(4,5)=\frac{e_{13}^{(j)}\left[c_{13}^{(j)}+p_je_{13}^{(j)}\right]\exp(-\mathrm{i}\alpha_{2j}\zeta_j)\left[-1+\exp(\mathrm{i}\alpha_{2j}\zeta_j)\right]^2}{2\left[c_{33}^{(j)}e_{13}^{(j)}-c_{13}^{(j)}e_{33}^{(j)}\right]},\quad T'_j(4,6)=0,$$

$$T'_j(5,1)=T'_j(5,2)=0,\quad T'_j(5,3)=\frac{\mathrm{i}\alpha_{2j}\left[c_{33}^{(j)}+p_je_{33}^{(j)}\right]\left[-\exp\left(-\mathrm{i}\alpha_{2j}\zeta_j\right)+\exp\left(\mathrm{i}\alpha_{2j}\zeta_j\right)\right]}{2},$$

$$T'_j(5,4)=\frac{e_{33}^{(j)}\left[c_{33}^{(j)}+p_je_{33}^{(j)}\right]\exp\left(-\mathrm{i}\alpha_{2j}\zeta_j\right)\left[-1+\exp\left(\mathrm{i}\alpha_{2j}\zeta_j\right)\right]^2}{2\left[-c_{33}^{(j)}e_{13}^{(j)}+c_{13}^{(j)}e_{33}^{(j)}\right]},$$

$$T'_j(5,5)=\frac{-2c_{13}^{(j)}e_{33}^{(j)}+e_{13}^{(j)}\exp\left(-i\alpha_{2j}\zeta_j\right)\left\{c_{33}^{(j)}\left[1+\exp\left(2i\alpha_{2j}\zeta_j\right)\right]+p_je_{33}^{(j)}\left[-1+\exp\left(i\alpha_{2j}\zeta_j\right)\right]^2\right\}}{2\left[c_{33}^{(j)}e_{13}^{(j)}-c_{13}^{(j)}e_{33}^{(j)}\right]},$$

$$T'_j(5,6)=0,\quad T'_j(6,1)=T'_j(6,2)=0,\quad T'_j(6,3)=\frac{p_j\exp\left(-i\alpha_{2j}\zeta_j\right)\left[-1+\exp\left(i\alpha_{2j}\zeta_j\right)\right]^2}{2},$$

$$T'_j(6,4)=\frac{ie_{33}^{(j)}p_j\left[-\exp\left(-i\alpha_{2j}\zeta_j\right)+\exp\left(i\alpha_{2j}\zeta_j\right)\right]}{2\alpha_{2j}\left[c_{33}^{(j)}e_{13}^{(j)}-c_{13}^{(j)}e_{33}^{(j)}\right]}+\frac{\zeta_j\left[c_{33}^{(j)}+p_je_{33}^{(j)}\right]}{c_{33}^{(j)}e_{13}^{(j)}-c_{13}^{(j)}e_{33}^{(j)}},$$

$$T'_j(6,5)=-\frac{ie_{13}^{(j)}p_j\left[-\exp\left(-i\alpha_{2j}\zeta_j\right)+\exp\left(i\alpha_{2j}\zeta_j\right)\right]}{2\alpha_{2j}\left[c_{33}^{(j)}e_{13}^{(j)}-c_{13}^{(j)}e_{33}^{(j)}\right]}-\frac{\zeta_j\left[c_{13}^{(j)}+p_je_{13}^{(j)}\right]}{c_{33}^{(j)}e_{13}^{(j)}-c_{13}^{(j)}e_{33}^{(j)}},$$

$$T'_j(6,6)=1.0,\quad (j=1,2). \tag{A.1}$$

References

[1] D.C. Hyland, L.D. Davis, Toward self-reliant control for adaptive structures, *Acta Astronautica* 51 (2002) 89–99.

[2] J.B. Castillero, J.A. Otero, R.R. Ramos, Asymptotic homogenization of laminated piezocomposite materials, *International Journal of Solids and Structures* 35 (1998) 527–541.

[3] L.P. Zinchuk, A.N. Podlipenets, Dispersion equations for Rayleigh waves in a piezoelectric periodically layered structure, *Journal of Mathematical Sciences* 103 (2001) 398–403.

[4] Z.H. Qian, F. Jin, Z.K. Wang, K. Kishimoto, Dispersion relations for SH-wave propagation in periodic piezoelectric composite layered structures, *International Journal of Engineering Science* 42 (2004) 673–689.

[5] A. Baz, Active control of periodic structures, *American Society of Mechanical Engineers Journal of Vibration and Acoustics* 123 (2001) 472–479.

[6] O. Thorp, M. Ruzzene, A. Baz, Attenuation and localization of wave propagation in rods with periodic shunted piezoelectric patches, *Smart Materials and Structures* 10 (2001) 979–989.

[7] F.M. Li, Y.S. Wang, C. Hu, W.H. Huang, Localization of elastic waves in randomly disordered multi-coupled multi-span beams, *Waves in Random Media* 14 (2004) 217–227.

[8] F.M. Li, Y.S. Wang, C. Hu, W.H. Huang, Localization of elastic waves in periodic rib-stiffened rectangular plates under axial compressive load, *Journal of Sound and Vibration* 281 (2005) 261–273.

[9] M.P. Castanier, C. Pierre, Lyapunov exponents and localization phenomena in multi-coupled nearly periodic systems, *Journal of Sound and Vibration* 183 (1995) 493–515.

[10] W.C. Xie, A. Ibrahim, Buckling mode localization in rib-stiffened plates with misplaced stiffeners—a finite strip approach, *Chaos, Solitons and Fractals* 11 (2000) 1543–1558.

[11] B. Gu, S.W. Yu, X.Q. Feng, Elastic wave scattering by an interface crack between a piezoelectric layer and elastic substrate, *International Journal of Fracture* 116 (2002) L29–L34.

[12] S. Ueda, Impact response of a piezoelectric layered composite plate with a crack, *Theoretical and Applied Fracture Mechanics* 38 (2002) 221–242.

[13] A. Wolf, J.B. Swift, H.L. Swinney, J.A. Vastano, Determining Lyapunov exponents from a time series, *Physica D* 16 (1985) 285–317.

[14] G.M. Odegard, Constitutive modeling of piezoelectric polymer composites, *Acta Materialia* 52 (2004) 5315–5330.

[15] G. Johansson, A.J. Niklasson, Approximate dynamic boundary conditions for a thin piezoelectric layer, *International Journal of Solids and Structures* 40 (2003) 3477–3492.